

# AdaptMMBench: Benchmarking Adaptive Multimodal Reasoning for Mode Selection and Reasoning Process

Xintong Zhang<sup>1,2,\*</sup> Xiaowen Zhang<sup>2,3,\*</sup> Jongrong Wu<sup>2,\*</sup> Zhi Gao<sup>1,2,4,†,♣</sup> Shilin Yan<sup>5,†</sup> Zhenxin Diao<sup>1,‡</sup>  
 Kunpeng Gao<sup>1,‡</sup> Xuanyan Chen<sup>1,‡</sup> Yuwei Wu<sup>1,4,♣</sup> Yunde Jia<sup>4</sup> Qing Li<sup>2,♣</sup>

<sup>1</sup>Beijing Key Laboratory of Intelligent Information Technology, School of Computer Science & Technology, Beijing Institute of Technology <sup>2</sup>State Key Laboratory of General Artificial Intelligence, BIGAI <sup>3</sup>Xidian University

<sup>4</sup>Guangdong Laboratory of Machine Perception and Intelligent Computing, Shenzhen MSU-BIT University <sup>5</sup>Alibaba Group

\* Core contribution, † Project supervisor, ‡ Equal contribution, ♣ Corresponding authors

Project Page: <https://adaptmmbench.github.io/>

## Abstract

Adaptive multimodal reasoning has emerged as a promising frontier in Vision-Language Models (VLMs), aiming to dynamically modulate between tool-augmented visual reasoning and text reasoning to enhance both effectiveness and efficiency. However, existing evaluations rely on static difficulty labels and simplistic metrics, which fail to capture the dynamic nature of difficulty relative to varying model capacities. Consequently, they obscure the distinction between adaptive mode selection and general performance while neglecting fine-grained process analyses. In this paper, we propose AdaptMMBench, a comprehensive benchmark for adaptive multimodal reasoning across five domains: real-world, OCR, GUI, knowledge, and math, encompassing both direct perception and complex reasoning tasks. AdaptMMBench utilizes a Matthews Correlation Coefficient (MCC) metric to evaluate the selection rationality of different reasoning modes, isolating this meta-cognition ability by dynamically identifying task difficulties based on models' capability boundaries. Moreover, AdaptMMBench facilitates multi-dimensional process evaluation across key step coverage, tool effectiveness, and computational efficiency. Our evaluation reveals that while adaptive mode selection scales with model capacity, it notably decouples from final accuracy. Conversely, key step coverage aligns with performance, though tool effectiveness remains highly inconsistent across model architectures.

Correspondence to: Zhi Gao <[gaozhi@bit.edu.cn](mailto:gaozhi@bit.edu.cn)>, Yuwei Wu <[yuwei.wu@bit.edu.cn](mailto:yuwei.wu@bit.edu.cn)>, Qing Li <[liqing@bigai.ai](mailto:liqing@bigai.ai)>.

Preprint. February 4, 2026.

## 1. Introduction

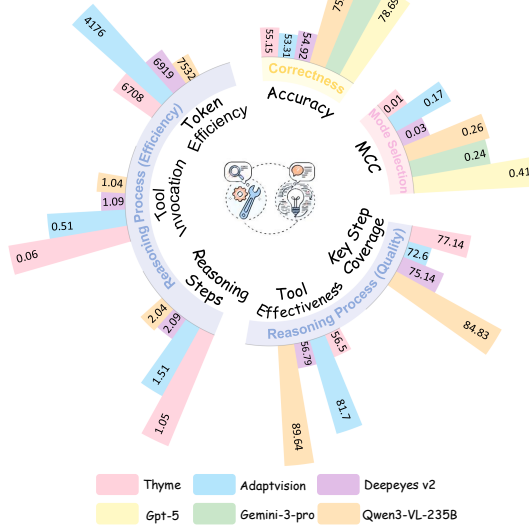


**Figure 1. Comparative Analysis of Accuracy, Reasoning Mode Selection, and Reasoning Process.** Closed-source models achieve stronger performance in accuracy and mode selection, while reasoning process quality is analyzed on open-source models due to limited access to closed-source reasoning traces.

Vision Language Models (VLMs) have evolved from passive observers of static visual inputs to proactive models capable of dynamic information seeking. This evolution makes a shift from direct perception and textual chain-of-thought (CoT) to the tool-augmented visual reasoning (i.e., thinking with images) (OpenAI, 2025), where models iteratively manipulate the visual content using visual tools, such as zoom-in, and enhancement(e.g., contrast and rotation) to acquire more visual information and resolve ambiguities. (Zheng et al., 2025; Hu et al., 2024). However, this capability introduces significant computational redundancy.

Lacking a mechanism to discern task necessity, models often fall into a ‘tool-invocation’ trap, applying intensive visual tools to tasks solvable by direct perception or text reasoning. Consequently, **adaptive multimodal reasoning** is a promising direction for VLMs, which balances the necessity of such tool-augmented visual reasoning against text reasoning (Lin et al., 2025b; Wang et al., 2025a).

Despite the emergence of adaptive multimodal reasoning formulations, **evaluating adaptive multimodal reasoning remains an open problem**. Most existing evaluations rely on token-level reduction, coarse tool-call statistics, or final accuracy as proxies for adaptive intelligence. While intuitive, these metrics primarily reflect observable outcomes rather than evaluating the internal reasoning process itself. In particular, they fail to disentangle adaptive reasoning mode selection from subsequent reasoning execution. The ability to select an appropriate reasoning mode is crucial, as it reflects difficulty-aware meta-cognition. From the data perspective, adaptive reasoning is commonly evaluated on domain-specific logic tasks (e.g., math and knowledge reasoning) or high-resolution perception benchmarks (Wu & Xie, 2024; Wang et al., 2025c; Zhang et al., 2025b). These benchmarks lack a hierarchy of difficulty, limiting their effectiveness in evaluating adaptive reasoning. Recent efforts such as Omni-AutoThink (Yang et al., 2025a) attempt to quantify adaptiveness through thinking rates under predefined difficulty levels, as shown in Fig. 2. While this encourages increased reasoning effort on harder tasks, predefined difficulty levels are not universally applicable across models, leading to evaluation bias. Moreover, existing evaluations largely overlook reasoning process quality, losing detailed analyzes to guide future multimodal reasoning research.

To bridge these gaps, we propose AdaptMMBench to quantify adaptive multimodal reasoning in VLMs. AdaptMMBench includes 1420 samples across five domains: real-world, OCR, GUI, knowledge, and math. Each domain contains both text-only solvable tasks and complex scenarios of varying difficulties requiring proactive visual tool invocation. AdaptMMBench enables separate evaluation of adaptive reasoning mode selection and the reasoning process. Specifically, it adopts the Matthews Correlation Coefficient (MCC) to evaluate mode selection by dynamically identifying task difficulties based on model performance boundaries. For reasoning process evaluation, we assess key step coverage, tool invocation effectiveness, and efficiency to measure reasoning coherence, tool correctness, and computational cost alongside accuracy.

We evaluate closed-source and open-source VLMs on AdaptMMBench, results shown in Fig. 1. Experiments reveal a relatively weak correlation between adaptive mode selection performance and final accuracy, whereas closed-source and larger models demonstrate stronger adaptive capability. By

contrast, key step coverage correlates more closely with accuracy, and tool execution effectiveness varies substantially across models.

Our contributions are summarized as follows.

- (1) We propose the AdaptMMBench to quantify the adaptive multimodal reasoning capabilities of VLMs, which contains 1420 samples across five domains with detailed reasoning annotations for comprehensive evaluations.
- (2) We establish a suite of metrics for adaptive multimodal reasoning, which disentangle the adaptive capability from other model capabilities and assess three aspects of the reasoning process, providing detailed and in-depth evaluations.
- (3) We analyze current VLMs from the perspective of adaptive reasoning, highlighting that the relationship between mode selection performance and final accuracy is relatively small, while closed-source and larger models exhibit stronger adaptive behavior. In contrast, key step coverage correlates more closely with accuracy, and tool execution effectiveness varies substantially across models.

## 2. Related Work

### 2.1. Multimodal Reasoning in VLMs

Early VLMs predominantly rely on text-only reasoning over fixed visual encodings, imposing a “first-glance” bottleneck that limits access to fine-grained visual details (Lu et al., 2023; Huang et al., 2025; Zhang et al., 2023; Yang et al., 2025b). Recent advanced models, including GPT-5 (Singh et al., 2025), Qwen3-VL (Bai et al., 2025), and InternVL (Zhu et al., 2025) have shifted multimodal reasoning from passive visual interpretation toward active, tool-augmented information seeking. Under this “thinking with images” paradigm, models acquire additional visual information through mechanisms such as multi-turn visual search (OpenAI, 2025; Zheng et al., 2025), region zoom-in (Wang et al., 2025b; Lai et al., 2025), and self-generated visual cues (Li et al., 2025a; Chern et al., 2025). In parallel, adaptive multimodal reasoning models have emerged to selectively invoke tools, trading off between text-only and tool-based reasoning to improve inference efficiency (Lin et al., 2025b; Zhang et al., 2025a; Wang et al., 2025a; Li et al., 2025d; e). More advanced systems further incorporate agentic workflows and code generation to support precise execution (Hong et al., 2025; Zhang et al., 2025c). While these works emphasize improvements in precision and efficiency, they offer limited evaluation of whether models invoke tool-based reasoning until text-only reasoning is insufficient, avoiding unnecessary computational overhead.

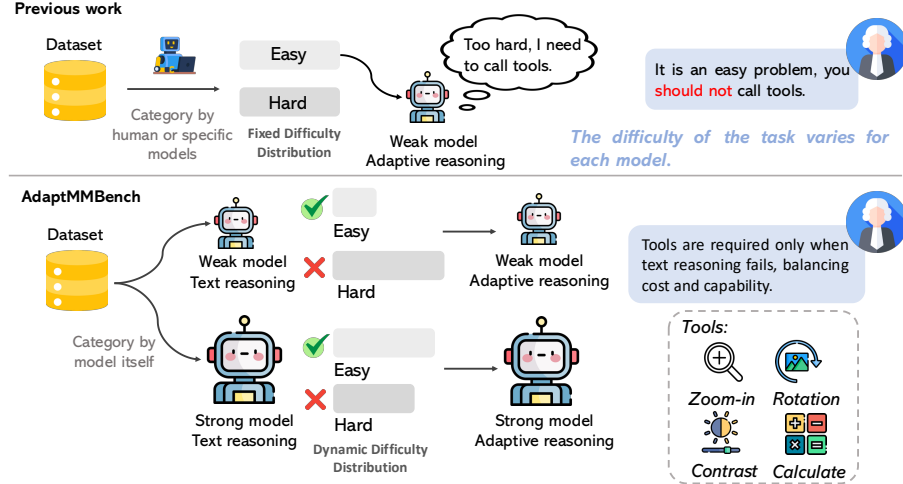


Figure 2. Illustration of our model-specific difficulty evaluation. Existing methods rely on static difficulty levels, while difficulty is inherently model-dependent.

## 2.2. Benchmarks for VLMs

Traditional VLM benchmarks mainly assess multimodal reasoning in structured domains with coarse visual content, such as chart understanding (Mathew et al., 2021; Masry et al., 2022), mathematical problem solving (Lu et al., 2023; Xiao et al., 2024), and other general-purpose VQA (Liu et al., 2024; Chen et al., 2024). MME-CoT (Jiang et al., 2025) further evaluates the correctness of the text reasoning process. As VLM capabilities improve, more recent benchmarks (Wu & Xie, 2024; Wang et al., 2025c) introduce higher-resolution images to better reflect complex conditions. Building on this trend, benchmarks such as VisualProbe (Lai et al., 2025), InSight-o3 (Li et al., 2025b), and TIR-Bench (Li et al., 2025c) emphasize fine-grained visual understanding and active visual reasoning through operations like region zoom-in and iterative exploration, implicitly requiring models to ‘thinking with images’. In parallel, generative benchmarks including VTBench (Lin et al., 2025a) and AuxSolidMath (Guo et al., 2025a) evaluate multimodal reasoning via self-produced auxiliary visual cues, extending visual reasoning beyond the information directly available in the input image. However, these visual-grounded benchmarks (Li et al., 2025b; Lin et al., 2025a) largely focus on task accuracy, overlooking the problem of redundant computation where models use visual tools for tasks already solvable through text-only reasoning. Relying solely on token reduction for efficiency evaluation fails to evaluate the adaptive decisions and the reasoning quality.

## 3. AdaptMMBench

AdaptMMBench focuses on two perspectives: adaptive reasoning mode selection and reasoning process.

## 3.1. Data Formulation

Formally, AdaptMMBench is constructed as a set of samples  $\mathcal{D} = \{d_i\}_{i=1}^N$ , where each data sample  $d_i$  is defined as:

$$d_i = (I, Q, A, E, K). \quad (1)$$

Here,  $I \in \mathbb{R}^{H \times W \times 3}$  denotes the input image,  $Q$  is the textual query, and  $A$  is the ground-truth answer. To support adaptive evaluation, we provide the visual tool annotation  $E$  that specifies how essential visual information can be obtained, including the coordinates of target regions as well as the required image transformations such as rotation and contrast adjustment.  $K = \{k_1, \dots, k_m\}$  is an ordered sequence of human-verified key reasoning steps describing the solution path from  $(I, Q)$  to  $A$ .

During inference, the model only observes the image  $I$  and the query  $Q$ . Acquiring the visual information specified by  $E$  requires invoking a visual tool  $t(I, \tau)$  via code execution or function calls, where  $t \in \mathcal{T}$  denotes a tool from the predefined toolset and  $\tau$  its execution arguments.

## 3.2. Data Collection

AdaptMMBench encompasses 1,420 samples spanning five domains: real-world, OCR, GUI, math, and knowledge, enabling a comprehensive evaluation of adaptive reasoning across diverse scenarios, as detailed in Fig. 3.

To ensure that AdaptMMBench contains both samples solvable via text-only reasoning and samples that require visual tool invocation under adaptive reasoning, we deliberately construct the dataset with diverse difficulty levels during data collection. One subset consists of samples solved by Qwen2.5-VL-7B under text-only reasoning. A second subset includes samples that Qwen2.5-VL-7B fails but can be



Figure 3. An Overview of AdaptMMBench. The benchmark contains data from five domains. Each domain includes samples requiring zoom-in and enhancement tools. We annotate zoom-in regions, enhancement arguments, and key reasoning steps.

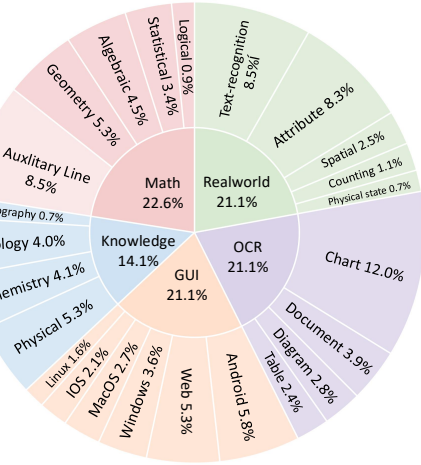


Figure 4. Domains and category of AdaptMMBench.

solved by Qwen3-VL-235B based on adaptive reasoning. A small portion remains unsolved even by Qwen3-VL-235B. The relative proportions of these three subsets are approximately 24%, 70%, and 6%. Notably, these subsets are introduced only to ensure difficulty diversity and do not determine the ground truth reasoning mode during evaluation. The reasoning mode selection label in adaptive mode

is made by the model itself, as detailed in Sec. 4.

Building on prior adaptive reasoning methods (Chern et al., 2025; Zhang et al., 2025c; Zhao et al., 2025), AdaptMMBench evaluates diverse visual tools beyond zoom-in, including geometric transformations for orientation correction and photometric adjustments for visual enhancement. During data construction, these requirements are induced via controlled distortions such as changes in contrast, brightness, and orientation, with zoom-in and transformation samples with a ratio of 5:2. We further include 120 samples requiring auxiliary-line generation, suggesting that reasoning with self-generated images constitutes an important extension of the think-with-images paradigm.

### 3.3. Annotation and Quality Control

#### Visual Tool & Key Step Annotation.

We collect initial data from existing benchmarks, with annotators providing bounding-box annotations for key regions, while visual enhancement annotations are generated through predefined transformations. Distortion parameters are constrained to maintain recoverability. GPT-5 is used to generate key reasoning steps  $K$ , which are manually verified. These components form annotated quintuples

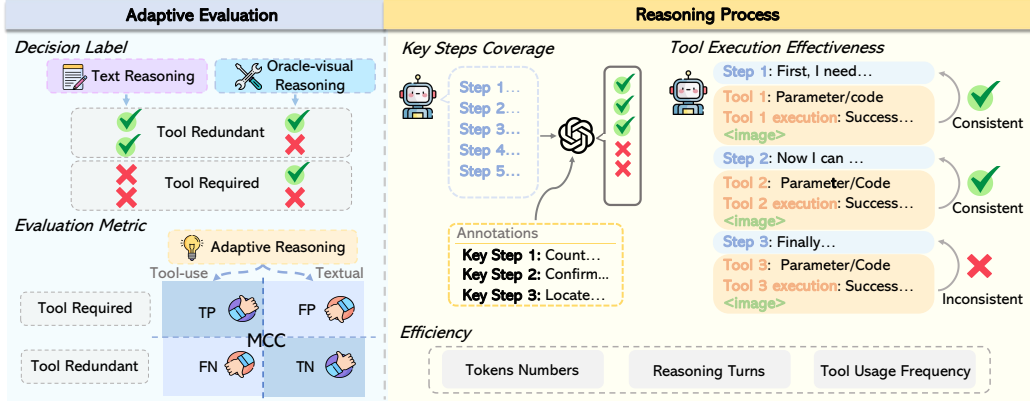


Figure 5. Evaluation pipeline for mode selection and reasoning process.

$(I, Q, A, E, K)$ .

**Quality Control.** Benchmark quality is ensured through a multi-stage verification pipeline. First, three independent annotators cross-validate each QA pair to remove ambiguity and verify correctness. Annotated image transformations and generated key reasoning steps are then reviewed by additional annotators for precision. Inaccurate instances are iteratively refined or re-annotated. This process ensures high-fidelity ground truth with precise pixel-level annotations and reliable key reasoning steps for comprehensively evaluating adaptive reasoning. More statistical information of AdaptMMBench can be found in Appendix A.

## 4. Evaluation Strategy

### 4.1. Evaluation Modes

Following the formulation defined in Sec. 3.1, we define three evaluation modes to systematically assess the model’s adaptive reasoning capabilities.

- **Text-Reasoning Mode:** Given  $(I, Q)$ , the model relies solely on text reasoning over the given image, without invoking active visual transformations, providing a baseline for assessing tool necessity.
- **Adaptive Reasoning Mode:** Given  $(I, Q)$ , the model adaptively selects between text-only reasoning and tool-augmented visual reasoning with tools. It generates a reasoning trajectory and records all tool invocation parameters, enabling evaluation of both its ability to decide when tool usage is required and the correctness of the reasoning process.
- **Oracle-Visual Mode:** Given  $(I, Q, I_E)$ , where  $I_E$  denotes gold-standard visual evidence from annotation  $E$ , the model performs text-only reasoning over the provided visual evidence, providing an upper-bound performance estimate under perfect visual acquisition.

### 4.2. Adaptive Mode Selection Evaluation

Adaptive intelligence depends on a model’s ability to assess whether its current information is sufficient to solve a task. Consequently, the appropriateness of a reasoning mode should be evaluated independently of answer correctness.

Under this principle, the necessity of tool invocation is determined by the outcome of text-only reasoning. If a task can be solved using text reasoning alone, it is labeled as **Tool-Redundant**, indicating that visual tool invocation is unnecessary and may introduce noise. Conversely, tasks that cannot be solved via text-only reasoning are labeled as **Tool-Required**, indicating that visual tool invocation is necessary to obtain additional information. This categorization defines the mode selection labels used in our evaluation, as detailed in Fig. 5. Accordingly, tool invocation decisions are evaluated using a confusion matrix: TP denotes Tool-Required cases where the model invokes tools, FN denotes Tool-Required cases where the model does not invoke tools, TN denotes Tool-Redundant cases where the model selects text-only reasoning, and FP denotes Tool-Redundant cases where the model unnecessarily invokes tools.

**Matthews Correlation Coefficient (MCC).** In adaptive mode selection, the proportions of tool-redundant and tool-required cases are model-dependent, leading to varying degrees of class imbalance in the resulting confusion matrix. To ensure a robust evaluation, we adopt the MCC,

$$MCC = \frac{TP \cdot TN - FP \cdot FN}{\sqrt{(TP + FP)(TP + FN)(TN + FP)(TN + FN)} + \epsilon}, \quad (2)$$

where  $\epsilon$  is a small constant for numerical stability. MCC ranges from  $[-1, 1]$ , with 1 indicating perfect agreement with the optimal mode selection, 0 denoting the chance-level performance, and  $-1$  indicating complete misalignment.

**Adaptive Label Robustness.** We analyze the effects of minor prompt variations on text and adaptive reasoning.

Only 0.02% of samples show inconsistent outcomes between text reasoning mode and text-only reasoning in adaptive mode. This indicates that the performance difference is stable under prompt variations, and adaptive reasoning rarely degrades text-solvable samples.

### 4.3. Reasoning Process Evaluation

While MCC measures the quality of mode selection, it does not assess the validity of the reasoning process. Models may produce correct answers despite logical errors or improper tool usage. To address this limitation, we introduce three process-oriented metrics to evaluate reasoning coherence and tool execution fidelity.

A reasoning trajectory  $\mathcal{R}$  is formalized as an interleaved sequence of reasoning steps and tool invocations:

$$\mathcal{R} = \{(s_1, t_1), (s_2, t_2), \dots, (s_n, t_n)\}, \quad (3)$$

where  $s_i$  is the reasoning at step  $i$  and  $t_i \in \mathcal{T}$  represents the corresponding tool invocation. The trajectory terminates at the final reasoning step  $s_n$ , and produces the answer.

#### 4.3.1. KEY STEPS COVERAGE

Following the evaluation paradigm of (Jiang et al., 2025), we assess whether a model’s reasoning chain  $\{s_i\}_{i=1}^n$  covers the essential human-annotated key steps  $K$  defined in Sec. 3.1. We employ GPT-5 as an evaluator to identify the presence of these key steps within the generated reasoning, and define the key step coverage as:

$$\text{KCoverage} = \frac{1}{|K|} \max_j \prod_{i=1}^j \mathbb{I}_{\text{GPT-5}}[k_i \in \{s_1, \dots, s_n\}]. \quad (4)$$

This metric measures how far the model’s reasoning progresses along the key steps. Rather than penalizing skipped or compressed steps, KCoverage captures the maximum extent to which the reasoning aligns with the solution structure, allowing different reasoning styles and reflecting how close the model comes to a correct solution.

#### 4.3.2. TOOL EXECUTION EFFECTIVENESS

To assess the precision of tool usage, we evaluate whether each tool invocation is semantically appropriate for its corresponding reasoning step and free of execution errors. The tool effectiveness is defined as:

$$\text{Effect}_{\text{tool}} = \frac{1}{N_{\text{tool}}} \sum_{i=1}^{N_{\text{tool}}} \text{valid}_{\text{GPT-5}}(t_i | s_i), \quad (5)$$

where  $N_{\text{tool}}$  denotes the total number of tool invocations,  $t_i \in \mathcal{T}$  is the tool invoked at step  $i$ , and  $\text{valid}_{\text{GPT-5}}(\cdot) \in \{0, 1\}$  is a semantic validity judgment provided by GPT-5.

#### 4.3.3. REASONING EFFICIENCY

Efficiency is evaluated in terms of token numbers, reasoning turns, and tool usage frequency, collectively capturing the conciseness of reasoning and the computational cost of adaptive execution.

*Table 1.* Evaluation of mode selection performance across models. We report TP, FP, TN, FN, and the MCC to assess meta-cognitive calibration in adaptive reasoning mode. Best and second-best scores in each category are highlighted in blue and green.

Model	TP ↑	FP ↓	TN ↑	FN ↓	MCC ↑
<i>Open-Source Models</i>					
PixelReasoner	280	196	434	390	0.11
DeepEyes	662	638	0	0	0.00
Thyme	20	20	655	605	0.01
PyVision	540	405	231	124	0.20
DeepEyes v2	623	676	1	0	0.03
AdaptVision	385	279	375	261	0.17
Qwen3-vl-8B-Instruct	328	381	351	240	0.06
Qwen3-vl-32B-Instruct	348	646	245	61	0.14
Qwen3-vl-235B-Instruct	286	437	487	90	0.26
<i>Closed-Source Models</i>					
GPT-5	482	392	376	50	<b>0.41</b>
Gemini-3-Pro	284	703	296	17	0.24

*Table 2.* Comprehensive evaluation of reasoning process, including key step coverage (Key Step Cov.), tool effectiveness (Tool Effect.), and efficiency. This assesses the logical rigor of the reasoning paths alongside their computational efficiency.

Model	Key Step Cov. (%) ↑	Tool Effect. (%) ↑	Efficiency		
			Steps ↓	Tools ↓	Tokens ↓
PixelReasoner	76.02	56.51	1.37	0.37	4229.00
DeepEyes	75.56	50.99	2.00	1.68	7601.45
Thyme	77.14	56.50	<b>1.05</b>	<b>0.06</b>	6708.47
PyVision	77.43	62.02	2.76	1.76	<b>2481.00</b>
DeepEyes v2	75.14	56.79	2.09	1.09	6918.90
AdaptVision	72.60	81.70	1.51	0.51	4175.96
Qwen3-vl-8B	78.40	91.62	1.76	1.20	8282.40
Qwen3-vl-32B	83.79	<b>92.98</b>	2.42	1.44	7725.99
Qwen3-vl-235B	<b>84.83</b>	89.64	2.04	1.04	7531.95

## 5. Experiments

We conduct a comprehensive quantitative evaluation of adaptive reasoning on AdaptMMBench, focusing on three complementary dimensions: (i) reasoning mode selection capability, (ii) quality and efficiency of reasoning process, and (iii) accuracy across reasoning modes.

### 5.1. Experiment Setting

We evaluate a set of VLMs to establish baselines for AdaptMMBench. For closed-source models, we select GPT-5 (Singh et al., 2025) and Gemini3 (Google DeepMind, 2025). For open-source models, we include the Qwen3-VL family (Bai et al., 2025) at multiple scales (8B, 32B, and 235B). In addition, we evaluate several specialized adaptive reasoning models, including DeepEyes (Zheng et al., 2025;

Table 3. Accuracy across different domains under three reasoning modes. Results are reported on 1,300 AdaptMMBench samples, with auxiliary-line tasks evaluated separately. \* indicates that the model supports enhancement operations. “w/o enh.” denotes results without enhancement-based data transformations (e.g., rotation and contrast).

Model	Mode	Real-world		OCR		GUI		Knowledge		Math (w/o aux)		Overall Accuracy	
		w/o enh.	All	w/o enh.	All	w/o enh.	All	w/o enh.	All	w/o enh.	All	w/o enh.	All
<i>Open-Source Models</i>													
PixelReasoner	Text	42.08	38.00	58.75	58.33	48.33	48.00	56.88	55.50	46.25	43.00	50.29	48.46
	Adaptive	53.75	51.33	61.25	62.33	61.67	53.00	58.13	59.00	51.88	50.00	55.19	55.23
	Oracle	70.83	67.67	72.92	75.00	66.67	58.67	65.62	67.50	62.50	64.00	65.96	66.69
Deepeyes	Text	50.00	48.33	50.42	51.33	52.50	53.33	50.62	48.50	43.12	41.50	49.71	49.15
	Adaptive	54.17	53.00	57.08	57.67	51.25	52.33	53.12	50.00	55.00	50.50	54.13	53.08
	Oracle	67.08	66.33	62.92	66.67	61.67	64.00	66.88	69.00	61.88	62.00	64.04	65.69
Thyme*	Text	55.00	51.67	58.33	57.67	50.00	49.67	55.00	51.00	51.88	48.00	54.13	51.92
	Adaptive	60.83	58.00	61.67	60.00	55.83	53.67	58.75	51.00	51.88	50.00	58.17	55.15
	Oracle	75.83	73.33	66.67	69.00	63.75	64.67	64.38	67.50	63.12	63.00	67.21	67.85
PyVision*	Text	40.00	38.00	62.08	60.33	75.00	70.00	35.62	34.50	35.00	31.00	51.73	48.92
	Adaptive	50.83	47.33	72.50	70.67	77.92	73.33	58.75	52.50	35.00	31.00	60.87	57.00
	Oracle	94.58	84.67	79.58	80.67	90.00	86.00	60.00	62.50	58.13	53.50	79.13	75.85
Deepeyes v2*	Text	58.75	55.00	58.33	58.33	54.58	54.67	48.12	47.50	41.88	39.00	53.46	52.08
	Adaptive	61.25	56.33	59.58	57.67	57.08	55.67	59.38	53.50	50.00	49.00	57.88	54.92
	Oracle	75.42	74.33	70.83	74.33	68.33	69.33	65.00	65.50	63.12	64.00	69.23	70.23
AdaptVision	Text	45.83	43.00	62.92	61.67	48.75	47.67	54.37	54.00	45.00	44.50	51.63	50.31
	Adaptive	49.17	46.33	64.17	64.00	52.92	54.33	60.62	54.50	49.38	45.00	55.29	53.31
	Oracle	74.17	70.67	71.25	76.00	62.92	65.67	71.88	73.00	68.75	69.00	69.71	70.85
Qwen3-vl-8B-Instruct	Text	56.25	50.00	64.17	62.33	57.50	54.00	72.50	66.00	55.62	50.50	60.77	56.31
	Adaptive	57.50	52.33	68.33	65.67	65.83	59.67	78.75	71.50	69.38	62.00	67.02	61.54
	Oracle	83.75	78.00	79.17	80.67	68.75	67.00	80.62	81.00	80.00	80.00	78.17	76.85
Qwen3-vl-32B-Instruct	Text	55.83	51.00	82.92	78.00	76.67	71.33	83.75	77.00	76.25	68.00	74.33	68.54
	Adaptive	63.33	57.33	85.42	82.67	77.00	70.00	84.38	79.00	81.88	73.50	77.79	71.92
	Oracle	87.08	81.67	92.92	92.00	81.67	75.67	96.25	95.00	90.00	87.50	89.04	85.62
Qwen3-vl-235B-Instruct	Text	59.58	52.33	81.25	78.00	84.58	76.67	83.12	78.50	83.12	73.00	77.60	71.08
	Adaptive	64.17	56.33	82.08	80.00	87.08	80.00	93.75	86.50	85.62	76.50	81.44	75.00
	Oracle	87.92	80.67	90.83	91.33	97.08	91.33	96.25	96.50	96.88	94.00	93.37	90.08
<i>Closed-Source Models</i>													
GPT-5*	Text	46.67	45.67	77.08	73.67	79.17	74.33	60.00	54.50	44.38	39.00	62.88	59.08
	Adaptive	70.83	64.67	89.17	86.33	88.75	85.33	92.50	86.00	76.88	71.00	83.46	78.69
	Oracle	97.92	88.00	90.42	90.00	91.67	88.00	96.88	94.50	90.62	83.00	93.46	88.69
Gemini-3-Pro*	Text	59.17	53.33	87.92	87.33	90.83	86.67	85.00	83.00	81.88	75.50	80.58	76.85
	Adaptive	80.42	74.00	89.58	89.67	92.08	90.00	92.50	93.50	93.12	87.00	89.04	86.31
	Oracle	87.50	80.33	92.59	93.00	94.17	92.67	92.50	94.00	93.75	91.00	91.92	89.85

Hong et al., 2025), PixelReasoner (Wang et al., 2025b), Thyme (Zhang et al., 2025c), PyVision (Zhao et al., 2025), and AdaptVision (Lin et al., 2025b). For all evaluated models, we follow the implementation details provided in their official codebases. For evaluations under different reasoning modes, we apply a unified and minimal modification to the prompts, as detailed in the Appendix D.

## 5.2. Adaptive Reasoning Mode Selection Capability

A closer analysis of mode selection capability reveals clear differences across models. As shown in Table 1 and Table 3, mode selection capability does not exhibit a strong correlation with final task accuracy. For example, AdaptVision achieves a relatively modest accuracy, yet demonstrates strong mode selection behavior with an MCC of 0.17, outperforming all other models trained on Qwen2.5-VL-7B

backbones. In contrast, GPT-5 attains the highest MCC of 0.41, demonstrating good mode selection capability.

**Model scaling improves mode selection.** Table 1 demonstrates a clear scaling trend within the Qwen3-VL family, where larger models exhibit more reliable mode selection. This pattern suggests that increased model capacity contributes to improved calibration when determining whether tool-based reasoning is necessary. Similarly, large-scale closed-source models outperform open-source models.

**Imbalanced mode selection behavior is observed in some models.** Several specialized adaptive models exhibit imbalanced mode selection behavior, either invoking tools excessively or rarely. For example, Deepeyes v2 invokes tools in all but one of the 1,300 samples in AdaptMMBench, whereas Thyme triggers tool usage in only about 3% of

cases. Such imbalanced patterns are associated with lower mode selection performance, despite competitive accuracy.

### 5.3. Quality and Efficiency of the Reasoning Process

Since intermediate reasoning steps of closed-source models (e.g., GPT-5 and Gemini-3-Pro) are not accessible, we restrict process-level analysis to open-source models. Table 2 evaluates key step coverage, tool effectiveness, and efficiency. Consistent with Table 3, key step coverage shows a similar ranking, with Qwen3-VL-235B among the top models. Larger models also demonstrate stronger tool effectiveness, better aligning tool usage with reasoning intent.

**Tool effectiveness varies with models.** Qwen3 family shows strong performance, while some smaller models are less effective. This may stem from repeated or unnecessary tool calls, as well as code-based tool invocation in Deepeyes v2, Thyme, and PyVision, which introduces more complexity than the function-call interface used by Qwen models.

**Token usage is not positively correlated with steps or tool calls.** Considering efficiency, token usage varies across models and does not correspond to the number of reasoning steps or tool calls. For example, Thyme uses the fewest steps and tool invocations, yet consumes more tokens than PyVision, which has the most steps. This shows that fewer steps or tool calls do not necessarily reduce token cost.

### 5.4. Accuracy across Reasoning Modes

We analyze model performance across different reasoning modes, including text-only, adaptive, and oracle tool reasoning. The oracle tool reflects upper-bound performance. As shown in Table 3, adaptive reasoning consistently improves accuracy over text-only baselines for all evaluated models.

**Significant performance gap between adaptive and oracle reasoning.** Although adaptive reasoning yields clear gains, oracle tool reasoning reveals substantial remaining headroom. For example, GPT-5 improves from 78.69% under adaptive reasoning to 88.69% in the oracle setting, with similar trends observed in open-source models. These results indicate that current performance is mainly limited by imperfect tool invocation rather than reasoning capability. Moreover, the high oracle-visual accuracy of 90.08% indicates the reliability and accuracy of our visual annotations.

**Generation-Based Tools Are Beneficial for Certain Tasks.** We conduct an exploratory analysis on self-generated auxiliary-line tasks as shown in Table 4. As current open-source models cannot generate visual representations, adaptive reasoning shows limited or negative gains over text-only reasoning, while oracle-visual inputs bring substantial improvements. This highlights the importance of visual generation for future adaptive reasoning models.

Table 4. Experimental results on geometric auxiliary-line problems across different reasoning modes.

Model	Text Acc	Adaptive Acc	Oracle Acc
<i>Open-Source VLMs</i>			
Thyme	21.67	21.67	24.17
PyVision	15.83	29.17	32.50
Deepeyes v2	19.17	19.17	25.83
Qwen3-vl-8B	50.00	46.67	62.50
Qwen3-vl-32B	63.33	58.33	79.17
Qwen3-vl-235B	62.50	68.33	84.17
<i>Closed-Source Models</i>			
Gemini-3-Pro	<b>85.00</b>	78.33	<b>94.17</b>
GPT-5	75.00	<b>86.67</b>	89.17

### 5.5. Error Analysis

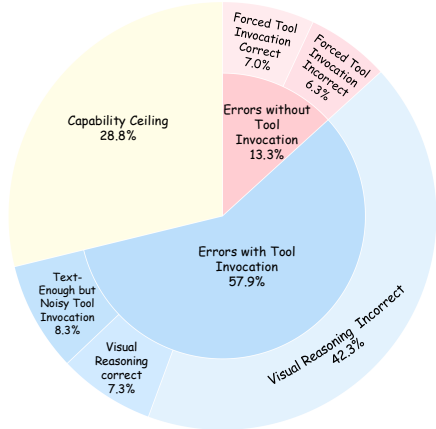


Figure 6. Error Analysis on GPT-5.

In this section, we analyze the causes of incorrect predictions made by GPT-5 under the adaptive mode to understand the gap between adaptive reasoning and oracle-visual mode. As shown in Fig. 6, most errors are related to tool usage. Specifically, 42.3% of the errors stem from visual reasoning failures, such as zoom-in into incorrect regions or applying wrong image transformations. Another 7.3% of errors occur even when visual reasoning is correct. Since these samples are solvable in the oracle-visual mode, this suggests that intermediate images in multi-step reasoning may introduce visual noise affecting the final prediction. In addition, 8.3% of errors are caused by incorrect mode selection, where text reasoning is sufficient but the model unnecessarily invokes tools, leading to degraded performance. For cases without tool usage, forcing tool invocation corrects 7.0% of the errors, while 6.3% remain incorrect. The remaining 28.8% of errors exceed the capability of the GPT-5 model.

## 6. Conclusion

In this paper, we present AdaptMMBench, a benchmark for evaluating adaptive multimodal reasoning in VLMs. AdaptMMBench covers diverse domains and reasoning

scenarios, and enables model-dependent identification of tool-redundant and tool-required cases by comparing performance across reasoning modes. We further propose a set of metrics that assess mode selection quality, reasoning process quality, and efficiency. Through systematic evaluation of state-of-the-art models, we observe that high accuracy does not necessarily imply strong reasoning mode selection capability. The substantial performance gap between adaptive and oracle-visual reasoning further suggests that performance is often limited by suboptimal tool invocation. This highlights adaptive tool selection as a key challenge for future multimodal reasoning models.

## Impact Statement

This paper presents work whose goal is to advance the field of Machine Learning. There are many potential societal consequences of our work, none which we feel must be specifically highlighted here.

## References

Bai, S., Cai, Y., Chen, R., Chen, K., Chen, X., Cheng, Z., Deng, L., Ding, W., Gao, C., Ge, C., Ge, W., Guo, Z., Huang, Q., Huang, J., Huang, F., Hui, B., Jiang, S., Li, Z., Li, M., Li, M., Li, K., Lin, Z., Lin, J., Liu, X., Liu, J., Liu, C., Liu, Y., Liu, D., Liu, S., Lu, D., Luo, R., Lv, C., Men, R., Meng, L., Ren, X., Ren, X., Song, S., Sun, Y., Tang, J., Tu, J., Wan, J., Wang, P., Wang, P., Wang, Q., Wang, Y., Xie, T., Xu, Y., Xu, H., Xu, J., Yang, Z., Yang, M., Yang, J., Yang, A., Yu, B., Zhang, F., Zhang, H., Zhang, X., Zheng, B., Zhong, H., Zhou, J., Zhou, F., Zhou, J., Zhu, Y., and Zhu, K. Qwen3-vl technical report. *arXiv preprint arXiv:2511.21631*, 2025.

Chen, L., Li, J., Dong, X., Zhang, P., Zang, Y., Chen, Z., Duan, H., Wang, J., Qiao, Y., Lin, D., et al. Are we on the right way for evaluating large vision-language models? *Advances in Neural Information Processing Systems*, 37: 27056–27087, 2024.

Chern, E., Hu, Z., Chern, S., Kou, S., Su, J., Ma, Y., Deng, Z., and Liu, P. Thinking with generated images. *arXiv preprint arXiv:2505.22525*, 2025.

Google DeepMind. A New Era of Intelligence with Gemini 3, 2025. URL <https://blog.google/products-and-platforms/products/gemini/gemini-3/>.

Guo, S., Pang, L., Wang, X., Wang, Y., Shen, H., and Zhang, J. Geovlmath: Enhancing geometry reasoning in vision-language models via cross-modal reward for auxiliary line creation. *arXiv preprint arXiv:2510.11020*, 2025a.

Guo, Z., Zhang, R., Chen, H., Gao, J., Jiang, D., Wang, J., and Heng, P.-A. Sciverse: Unveiling the knowledge comprehension and visual reasoning of lmms on multimodal scientific problems. In *Findings of the Association for Computational Linguistics: ACL 2025*, pp. 19683–19704, 2025b.

Hong, J., Zhao, C., Zhu, C., Lu, W., Xu, G., and Yu, X. Deepeyesv2: Toward agentic multimodal model. *arXiv preprint arXiv:2511.05271*, 2025.

Hu, Y., Shi, W., Fu, X., Roth, D., Ostendorf, M., Zettlemoyer, L., Smith, N. A., and Krishna, R. Visual sketchpad: Sketching as a visual chain of thought for multimodal language models. *Advances in Neural Information Processing Systems*, 37:139348–139379, 2024.

Huang, W., Jia, B., Zhai, Z., Cao, S., Ye, Z., Zhao, F., Xu, Z., Hu, Y., and Lin, S. Vision-r1: Incentivizing reasoning capability in multimodal large language models. *arXiv preprint arXiv:2503.06749*, 2025.

Jiang, D., Zhang, R., Guo, Z., Li, Y., Qi, Y., Chen, X., Wang, L., Jin, J., Guo, C., Yan, S., et al. Mme-cot: Benchmarking chain-of-thought in large multimodal models for reasoning quality, robustness, and efficiency. *arXiv preprint arXiv:2502.09621*, 2025.

Kirillov, A., Mintun, E., Ravi, N., Mao, H., Rolland, C., Gustafson, L., Xiao, T., Whitehead, S., Berg, A. C., Lo, W.-Y., et al. Segment anything. In *Proceedings of the IEEE/CVF international conference on computer vision*, pp. 4015–4026, 2023.

Lai, X., Li, J., Li, W., Liu, T., Li, T., and Zhao, H. Mini-o3: Scaling up reasoning patterns and interaction turns for visual search. *arXiv preprint arXiv:2509.07969*, 2025.

Li, C., Wu, W., Zhang, H., Xia, Y., Mao, S., Dong, L., Vulić, I., and Wei, F. Imagine while reasoning in space: Multimodal visualization-of-thought. *arXiv preprint arXiv:2501.07542*, 2025a.

Li, K., Yao, L., Wu, J., Yu, T., Chen, J., Bai, H., Hou, L., Hong, L., Zhang, W., and Zhang, N. L. Insight-o3: Empowering multimodal foundation models with generalized visual search. *arXiv preprint arXiv:2512.18745*, 2025b.

Li, M., Zhong, J., Zhao, S., Zhang, H., Lin, S., Lai, Y., Wei, C., Psounis, K., and Zhang, K. Tir-bench: A comprehensive benchmark for agentic thinking-with-images reasoning. *arXiv preprint arXiv:2511.01833*, 2025c.

Li, X., Li, X., Gao, J., Pi, R., Hu, S., and Zhang, W. Look less, reason more: Rollout-guided adaptive pixel-space reasoning. *arXiv preprint arXiv:2510.01681*, 2025d.

Li, Z., Zhao, Y., Zhang, J., Wang, S., Yao, Y., Zhao, R., Song, J., Zheng, B., and Wei, Z. Mixture-of-visual-thoughts: Exploring context-adaptive reasoning mode selection for general visual reasoning. *arXiv preprint arXiv:2509.22746*, 2025e.

Lin, H., Geng, T., Xu, Z., and Zhao, W. Vtbench: Evaluating visual tokenizers for autoregressive image generation. *arXiv preprint arXiv:2505.13439*, 2025a.

Lin, Z., Liu, Y., Yang, Y., Tao, L., and Ye, D. Adaptvision: Efficient vision-language models via adaptive visual acquisition. *arXiv preprint arXiv:2512.03794*, 2025b.

Liu, Y., Duan, H., Zhang, Y., Li, B., Zhang, S., Zhao, W., Yuan, Y., Wang, J., He, C., Liu, Z., et al. Mmbench: Is your multi-modal model an all-around player? In *European conference on computer vision*, pp. 216–233. Springer, 2024.

Lu, P., Bansal, H., Xia, T., Liu, J., Li, C., Hajishirzi, H., Cheng, H., Chang, K.-W., Galley, M., and Gao, J. Mathvista: Evaluating mathematical reasoning of foundation models in visual contexts. *arXiv preprint arXiv:2310.02255*, 2023.

Masry, A., Do, X. L., Tan, J. Q., Joty, S., and Hoque, E. Chartqa: A benchmark for question answering about charts with visual and logical reasoning. In *Findings of the association for computational linguistics: ACL 2022*, pp. 2263–2279, 2022.

Masry, A., Islam, M. S., Ahmed, M., Bajaj, A., Kabir, F., Kartha, A., Laskar, M. T. R., Rahman, M., Rahman, S., Shahmohammadi, M., et al. Chartqapro: A more diverse and challenging benchmark for chart question answering. *arXiv preprint arXiv:2504.05506*, 2025.

Mathew, M., Karatzas, D., and Jawahar, C. Docvqa: A dataset for vqa on document images. In *Proceedings of the IEEE/CVF winter conference on applications of computer vision*, pp. 2200–2209, 2021.

OpenAI. Openai o3 and o4-mini system card. Technical report, OpenAI, 2025. URL <https://cdn.openai.com/pdf/2221c875-02dc-4789-800b-e7758f3722c1/o3-and-o4-mini-system-card.pdf>.

Qiao, R., Tan, Q., Dong, G., MinhuiWu, M., Sun, C., Song, X., Wang, J., Gongque, Z., Lei, S., Zhang, Y., et al. Wemath: Does your large multimodal model achieve human-like mathematical reasoning? In *Proceedings of the 63rd Annual Meeting of the Association for Computational Linguistics (Volume 1: Long Papers)*, pp. 20023–20070, 2025.

Shi, C., Yu, Z., Gao, Z., Feng, R., Liu, E., Wu, Y., Jia, Y., Xiang, L., He, Z., and Li, Q. Gui knowledge bench: Revealing the knowledge gap behind vlm failures in gui tasks. *arXiv preprint arXiv:2510.26098*, 2025.

Singh, A., Fry, A., Perelman, A., Tart, A., Ganesh, A., El-Kishky, A., McLaughlin, A., Low, A., Ostrow, A., Ananthram, A., et al. Openai gpt-5 system card. *arXiv preprint arXiv:2601.03267*, 2025.

Wang, C., Feng, K., Chen, D., Wang, Z., Li, Z., Gao, S., Meng, M., Zhou, X., Zhang, M., Shang, Y., et al. Adatooler-v: Adaptive tool-use for images and videos. *arXiv preprint arXiv:2512.16918*, 2025a.

Wang, H., Su, A., Ren, W., Lin, F., and Chen, W. Pixel reasoner: Incentivizing pixel-space reasoning with curiosity-driven reinforcement learning. *arXiv preprint arXiv:2505.15966*, 2025b.

Wang, W., Ding, L., Zeng, M., Zhou, X., Shen, L., Luo, Y., Yu, W., and Tao, D. Divide, conquer and combine: A training-free framework for high-resolution image perception in multimodal large language models. In *Proceedings of the AAAI Conference on Artificial Intelligence*, volume 39, pp. 7907–7915, 2025c.

Wu, J., Yin, W., Jiang, Y., Wang, Z., Xi, Z., Fang, R., Zhang, L., He, Y., Zhou, D., Xie, P., et al. Webwalker: Benchmarking llms in web traversal. *arXiv preprint arXiv:2501.07572*, 2025.

Wu, P. and Xie, S. V?: Guided visual search as a core mechanism in multimodal llms. In *Proceedings of the IEEE/CVF Conference on Computer Vision and Pattern Recognition*, pp. 13084–13094, 2024.

Xiao, Y., Sun, E., Liu, T., and Wang, W. Logicvista: Multimodal llm logical reasoning benchmark in visual contexts. *arXiv preprint arXiv:2407.04973*, 2024.

Xu, W., Wang, J., Wang, W., Chen, Z., Zhou, W., Yang, A., Lu, L., Li, H., Wang, X., Zhu, X., et al. Visulogic: A benchmark for evaluating visual reasoning in multi-modal large language models. *arXiv preprint arXiv:2504.15279*, 2025.

Yang, D., Liu, S., Wang, D., Wang, Y., Wan, G., and Meng, H. Omni-autothink: Adaptive multimodal reasoning via reinforcement learning. *arXiv preprint arXiv:2512.03783*, 2025a.

Yang, S., Han, C., Luo, S., and Hovy, E. Magic-vqa: Multimodal and grounded inference with commonsense knowledge for visual question answering. In *Findings of the Association for Computational Linguistics: ACL 2025*, pp. 16967–16986, 2025b.

Yue, X., Ni, Y., Zhang, K., Zheng, T., Liu, R., Zhang, G., Stevens, S., Jiang, D., Ren, W., Sun, Y., et al. Mmmu: A massive multi-discipline multimodal understanding and reasoning benchmark for expert agi. In *Proceedings of the IEEE/CVF Conference on Computer Vision and Pattern Recognition*, pp. 9556–9567, 2024.

Zhang, R., Jiang, D., Zhang, Y., Lin, H., Guo, Z., Qiu, P., Zhou, A., Lu, P., Chang, K.-W., Qiao, Y., et al. Mathverse: Does your multi-modal llm truly see the diagrams in visual math problems? In *European Conference on Computer Vision*, pp. 169–186. Springer, 2024.

Zhang, X., Gao, Z., Zhang, B., Li, P., Zhang, X., Liu, Y., Yuan, T., Wu, Y., Jia, Y., Zhu, S.-C., et al. Chain-of-focus: Adaptive visual search and zooming for multimodal reasoning via rl. *arXiv preprint arXiv:2505.15436*, 2025a.

Zhang, Y., Zhang, H., Tian, H., Fu, C., Zhang, S., Wu, J., Li, F., Wang, K., Wen, Q., Zhang, Z., Wang, L., and Jin, R. Mme-realworld: Could your multimodal LLM challenge high-resolution real-world scenarios that are difficult for humans? In *The Thirteenth International Conference on Learning Representations (ICLR)*, 2025b.

Zhang, Y.-F., Lu, X., Yin, S., Fu, C., Chen, W., Hu, X., Wen, B., Jiang, K., Liu, C., Zhang, T., et al. Thyme: Think beyond images. *arXiv preprint arXiv:2508.11630*, 2025c.

Zhang, Z., Zhang, A., Li, M., Zhao, H., Karypis, G., and Smola, A. Multimodal chain-of-thought reasoning in language models. *arXiv preprint arXiv:2302.00923*, 2023.

Zhao, S., Zhang, H., Lin, S., Li, M., Wu, Q., Zhang, K., and Wei, C. Pyvision: Agentic vision with dynamic tooling. *arXiv preprint arXiv:2507.07998*, 2025.

Zheng, Z., Yang, M., Hong, J., Zhao, C., Xu, G., Yang, L., Shen, C., and Yu, X. Deepeyes: Incentivizing” thinking with images” via reinforcement learning. *arXiv preprint arXiv:2505.14362*, 2025.

Zhu, J., Wang, W., Chen, Z., Liu, Z., Ye, S., Gu, L., Tian, H., Duan, Y., Su, W., Shao, J., et al. Internvl3: Exploring advanced training and test-time recipes for open-source multimodal models. *arXiv preprint arXiv:2504.10479*, 2025.

## A. More Data Details

### A.1. Data Source Distribution

**Real-World VQA.** We target high-resolution natural scenes by leveraging VisualProbe (Lai et al., 2025) for small-object search and a custom SA-1B (Kirillov et al., 2023) subset for large-scale object reasoning. Queries are explicitly designed to evaluate attributes, spatial, counting, physical state and text-recognition across distinct scales. Moreover, statistics of bounding box sizes are presented in Fig. 7.

**Text-Rich VQA.** This domain covers diverse charts, tables, and documents. We aggregate standard samples from ChartQA (Masry et al., 2022) and DocVQA (Mathew et al., 2021) with high-resolution challenges from ChartQA-Pro (Masry et al., 2025), MM-RealWorld (Zhang et al., 2025b), and Insight-o3 (Li et al., 2025b) to demand precise visual inspection and deep reasoning.

**Math VQA.** To assess mathematical reasoning in visual contexts, we consolidate high-quality samples from a spectrum of established benchmarks including MathVista (Lu et al., 2023), MathVerse (Zhang et al., 2024), We-Math (Qiao et al., 2025), LogicVista (Xiao et al., 2024), Visulogic (Xu et al., 2025), AuxSolidMath, and VTBench (Lin et al., 2025a).

**GUI VQA.** We construct a cross-platform suite covering iOS, Android, Web, macOS, Windows, and Linux. This is achieved by integrating generic datasets like GUI-Knowledge-Bench (Shi et al., 2025) and MMBench-GUI (Liu et al., 2024) with domain-specific samples from WebWalker (Wu et al., 2025).

**Knowledge VQA.** This category is sourced from disciplinary benchmarks across Physics, Chemistry, and Biology. Specifically, we incorporate expert-level samples from MMMU (Yue et al., 2024) and SciVerse (Guo et al., 2025b) to evaluate the models’ ability to integrate specialized domain knowledge with visual reasoning.

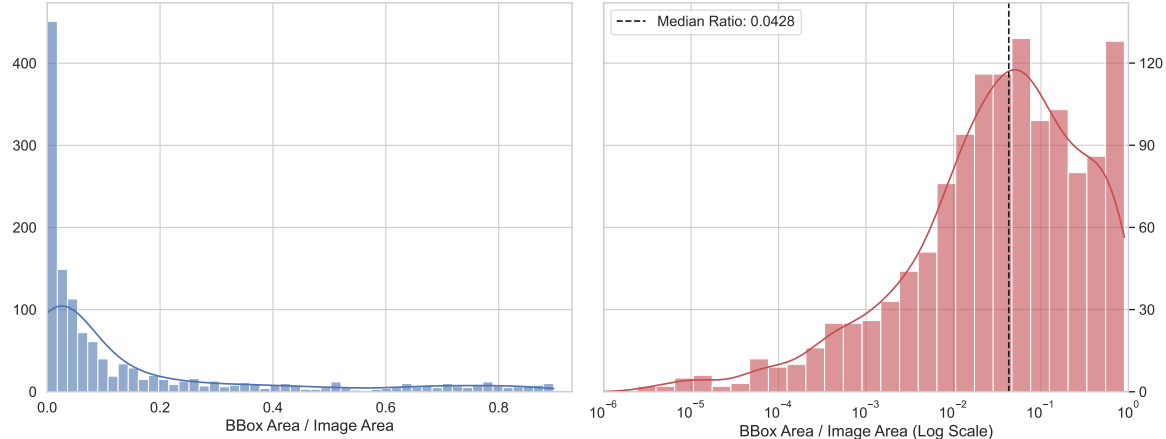


Figure 7. Statistics of bounding box sizes in AdaptMMBench.

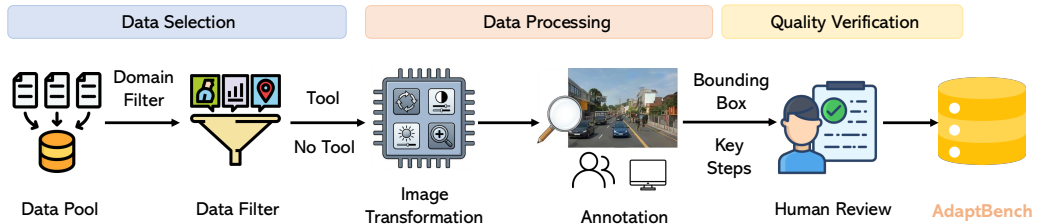


Figure 8. Overview of the data curation and annotation process.

### A.2. Data Construction Pipeline

The construction workflow of AdaptBench is depicted in Figure 8. Initially, raw data is partitioned based on reasoning complexity, specifically separating tasks that necessitate external tool intervention from those amenable to text-only inference.

To further challenge model adaptability, we augment the visual inputs with diverse transformations, thereby mandating fine-grained perception. Finally, we implement a multi-stage verification pipeline involving expert annotation of transformation logic, key reasoning steps, and rigorous human review, ensuring a high-fidelity ground truth for the final benchmark.

## B. Transform Results

Tab. 5 serves as a supplementary detailed analysis to the main experimental results presented in Tab. 3. While Tab. 3 reports the model performance on the original dataset (denoted as “w/o enh.”) and the aggregated dataset (“All”), it does not explicitly isolate the performance on the transformed data. To provide a comprehensive view of model robustness against data variations, Tab. 5 exclusively presents the accuracy results for the **Transformed** subset across all five domains. The highlighting scheme follows the same convention as the main table to facilitate direct comparison of the autonomous decision-making capabilities in the Adaptive mode.

*Table 5.* Main experimental results on the **Transform** subset of AdaptBench. We report accuracy (%) across five specific domains and overall aggregates. Performance for **Text** and **Oracle** modes is displayed in deep gray to prioritize adaptive results. \* indicates that the model supports enhancement operations.

Model	Mode	Real-world	OCR	GUI	Knowledge	Math	Overall Accuracy
<i>Open-Source Models</i>							
PixelReasoner	Text	46.67	50.00	30.00	56.67	21.67	41.15
	Adaptive	61.67	62.50	42.50	66.67	41.67	55.38
	Oracle	66.67	75.00	70.00	83.33	55.00	69.62
Deepeyes	Text	56.67	40.00	35.00	55.00	41.67	46.92
	Adaptive	56.67	37.50	32.50	60.00	48.33	48.85
	Oracle	73.33	77.50	65.00	81.67	63.33	72.31
Thyme*	Text	48.33	35.00	32.50	55.00	38.33	43.08
	Adaptive	45.00	20.00	42.50	53.33	46.67	43.08
	Oracle	68.33	80.00	62.50	78.33	63.33	70.38
PyVision*	Text	50.00	30.00	15.00	53.33	30.00	37.69
	Adaptive	55.00	27.50	15.00	63.33	33.33	41.54
	Oracle	70.00	72.50	35.00	85.00	45.00	62.69
Deepeyes v2*	Text	55.00	45.00	27.50	58.33	40.00	46.54
	Adaptive	50.00	30.00	45.00	50.00	36.67	43.08
	Oracle	73.33	67.50	67.50	88.33	70.00	74.23
AdaptVision	Text	43.33	52.50	42.50	56.67	31.67	45.00
	Adaptive	60.00	30.00	27.50	63.33	35.00	45.38
	Oracle	76.67	77.50	70.00	95.00	56.67	75.38
Qwen3-VL-8B-Instruct	Text	40.00	40.00	30.00	55.00	25.00	38.46
	Adaptive	35.00	42.50	32.50	55.00	31.67	39.62
	Oracle	60.00	82.50	80.00	86.67	55.00	71.54
Qwen3-VL-32B-Instruct	Text	50.00	50.00	35.00	58.33	31.67	45.38
	Adaptive	40.00	57.50	40.00	71.67	33.33	48.46
	Oracle	51.67	90.00	77.50	88.33	60.00	71.92
Qwen3-VL-235B-Instruct	Text	45.00	60.00	32.50	65.00	23.33	45.00
	Adaptive	51.67	57.50	40.00	71.67	25.00	49.23
	Oracle	68.33	97.50	82.50	93.33	51.67	76.92
<i>Closed-Source Models</i>							
GPT-5*	Text	55.00	32.50	17.50	60.00	41.67	43.85
	Adaptive	71.67	60.00	47.50	75.00	40.00	59.62
	Oracle	73.33	85.00	52.50	88.33	48.33	69.62
Gemini-3-Pro*	Text	70.00	75.00	50.00	85.00	30.00	61.92
	Adaptive	81.67	97.50	62.50	90.00	48.33	75.38
	Oracle	86.67	100.00	80.00	95.00	51.67	81.54

## C. Category Results

In this section, we provide a fine-grained analysis of model performance across all specific categories defined in our benchmark. To ensure legibility and accommodate the wide range of sub-domains, the detailed accuracy results are presented in two separate tables:

- **Tab. 6** reports the performance metrics for the **GUI** and **Realworld** domains.
- **Tab. 7** covers the **Knowledge**, **Math**, and **OCR** domains.

In both tables, the first row (labeled as  $N$ ) denotes the number of test samples available for each corresponding category. All accuracy values are reported in decimal format.

Table 6. Detailed Accuracy (Part 1/2): GUI and Realworld domains. \* indicates that the model supports enhancement operations.

Model	Mode	GUI						Realworld				
		And.	Lin.	Mac.	Web	Win.	iOS	Attr.	Count	Integ.	Phys.	Spat.
$N$	(Count)	83	22	39	75	51	30	118	16	121	10	35
PixelReasoner	Text	0.51	0.45	0.31	0.52	0.53	0.47	0.45	0.12	0.35	0.50	0.34
	Adaptive	0.51	0.50	0.41	0.61	0.57	0.50	0.55	0.50	0.49	0.70	0.43
	Oracle	0.59	0.68	0.36	0.63	0.67	0.57	0.68	0.75	0.69	0.50	0.63
Deepeyes	Text	0.59	0.45	0.36	0.63	0.45	0.57	0.55	0.38	0.44	0.30	0.51
	Adaptive	0.48	0.36	0.44	0.68	0.49	0.53	0.58	0.44	0.50	0.30	0.57
	Oracle	0.67	0.50	0.46	0.75	0.63	0.63	0.65	0.69	0.69	0.40	0.69
Thyme*	Text	0.53	0.45	0.36	0.60	0.41	0.50	0.57	0.62	0.51	0.40	0.34
	Adaptive	0.54	0.55	0.41	0.64	0.45	0.57	0.64	0.75	0.54	0.40	0.51
	Oracle	0.61	0.68	0.56	0.80	0.55	0.60	0.73	0.75	0.79	0.60	0.60
PyVision*	Text	0.81	0.64	0.82	0.47	0.76	0.77	0.51	0.44	0.24	0.40	0.40
	Adaptive	0.83	0.59	0.82	0.51	0.80	0.90	0.58	0.44	0.36	0.50	0.51
	Oracle	0.92	0.77	0.92	0.79	0.88	0.83	0.87	0.88	0.80	0.70	0.94
Deepeyes v2*	Text	0.46	0.45	0.46	0.68	0.59	0.57	0.60	0.50	0.52	0.70	0.46
	Adaptive	0.49	0.45	0.44	0.71	0.53	0.63	0.58	0.69	0.55	0.50	0.49
	Oracle	0.64	0.68	0.51	0.77	0.76	0.77	0.72	0.81	0.79	0.80	0.63
AdaptVision	Text	0.48	0.32	0.28	0.59	0.49	0.53	0.48	0.25	0.40	0.60	0.40
	Adaptive	0.51	0.36	0.41	0.68	0.55	0.60	0.54	0.25	0.40	0.60	0.46
	Oracle	0.65	0.50	0.51	0.76	0.71	0.63	0.69	0.69	0.75	0.80	0.60
Qwen3-VL-8B-Instruct	Text	0.52	0.45	0.49	0.64	0.51	0.53	0.55	0.44	0.47	0.70	0.40
	Adaptive	0.61	0.64	0.46	0.63	0.57	0.67	0.58	0.50	0.44	0.70	0.57
	Oracle	0.70	0.59	0.51	0.77	0.67	0.60	0.70	0.88	0.84	0.80	0.77
Qwen3-VL-32B-Instruct	Text	0.81	0.77	0.56	0.75	0.57	0.77	0.56	0.56	0.50	0.50	0.34
	Adaptive	0.76	0.77	0.51	0.68	0.67	0.83	0.64	0.50	0.54	0.80	0.46
	Oracle	0.80	0.68	0.62	0.83	0.73	0.77	0.78	0.81	0.86	0.70	0.83
Qwen3-VL-235B-Instruct	Text	0.80	0.77	0.79	0.65	0.88	0.73	0.61	0.50	0.50	0.40	0.34
	Adaptive	0.83	0.77	0.87	0.76	0.78	0.77	0.60	0.50	0.57	0.50	0.46
	Oracle	0.92	0.91	0.95	0.88	0.94	0.90	0.81	0.75	0.83	0.60	0.83
GPT-5*	Text	0.86	0.82	0.87	0.47	0.75	0.90	0.62	0.44	0.31	0.40	0.46
	Adaptive	0.89	0.86	0.90	0.75	0.88	0.90	0.77	0.62	0.55	0.60	0.57
	Oracle	0.96	0.95	0.82	0.84	0.80	0.90	0.92	0.88	0.82	0.80	0.97
Gemini-3-Pro*	Text	0.90	0.86	0.92	0.79	0.86	0.90	0.58	0.38	0.50	0.50	0.54
	Adaptive	0.93	0.86	0.95	0.84	0.90	0.93	0.82	0.69	0.69	0.90	0.60
	Oracle	0.94	0.91	0.97	0.91	0.90	0.93	0.83	0.75	0.78	0.70	0.86

Table 7. Detailed Accuracy (Part 2/2): Knowledge, Math, and OCR domains. \* indicates that the model supports enhancement operations.

Model	Mode	Knowledge				Math				OCR			
		Bio.	Chem.	Geo.	Phys.	Alg.	Geo.	Log.	Stat.	Chart	Diag.	Doc.	Tab.
<i>N</i>	(Count)	57	58	10	75	64	75	13	48	171	40	55	34
PixelReasoner	Text	0.68	0.47	0.70	0.51	0.44	0.44	0.38	0.42	0.57	0.70	0.53	0.62
	Adaptive	0.70	0.45	0.50	0.63	0.52	0.49	0.38	0.52	0.65	0.62	0.55	0.62
	Oracle	0.82	0.62	0.60	0.61	0.69	0.69	0.46	0.54	0.72	0.88	0.73	0.79
Deepeyes	Text	0.61	0.38	0.70	0.44	0.45	0.48	0.31	0.29	0.49	0.52	0.51	0.62
	Adaptive	0.65	0.40	0.70	0.44	0.47	0.59	0.31	0.48	0.58	0.62	0.55	0.53
	Oracle	0.79	0.66	1.00	0.60	0.66	0.64	0.54	0.58	0.63	0.78	0.64	0.76
Thyme*	Text	0.65	0.40	0.70	0.47	0.53	0.52	0.31	0.40	0.56	0.55	0.55	0.76
	Adaptive	0.67	0.41	0.60	0.45	0.52	0.53	0.54	0.42	0.61	0.57	0.56	0.65
	Oracle	0.75	0.66	0.90	0.60	0.64	0.73	0.38	0.52	0.69	0.75	0.62	0.74
PyVision*	Text	0.51	0.16	0.60	0.33	0.28	0.33	0.38	0.29	0.59	0.62	0.58	0.68
	Adaptive	0.72	0.36	0.60	0.49	0.25	0.39	0.31	0.27	0.72	0.75	0.64	0.71
	Oracle	0.56	0.74	0.70	0.57	0.48	0.52	0.46	0.65	0.74	0.85	0.87	0.97
Deepeyes v2*	Text	0.60	0.43	0.30	0.44	0.48	0.40	0.15	0.31	0.58	0.68	0.51	0.62
	Adaptive	0.65	0.48	0.50	0.49	0.50	0.57	0.31	0.40	0.61	0.55	0.51	0.53
	Oracle	0.84	0.53	0.50	0.63	0.66	0.69	0.31	0.62	0.74	0.80	0.73	0.71
AdaptVision	Text	0.63	0.47	0.70	0.51	0.41	0.59	0.15	0.35	0.59	0.70	0.58	0.71
	Adaptive	0.61	0.55	0.80	0.45	0.45	0.52	0.46	0.33	0.63	0.65	0.64	0.68
	Oracle	0.84	0.67	0.90	0.67	0.70	0.72	0.46	0.69	0.70	0.98	0.78	0.76
Qwen3-VL-8B-Instruct	Text	0.75	0.62	0.40	0.65	0.55	0.47	0.31	0.56	0.65	0.75	0.36	0.76
	Adaptive	0.75	0.71	0.70	0.69	0.69	0.56	0.38	0.69	0.68	0.70	0.53	0.71
	Oracle	0.91	0.79	0.60	0.77	0.86	0.77	0.38	0.88	0.78	0.98	0.69	0.91
Qwen3-VL-32B-Instruct	Text	0.84	0.78	1.00	0.68	0.67	0.68	0.31	0.79	0.81	0.82	0.62	0.82
	Adaptive	0.82	0.76	0.90	0.77	0.67	0.77	0.38	0.85	0.83	0.90	0.75	0.85
	Oracle	0.95	0.95	0.90	0.96	0.95	0.84	0.38	0.96	0.91	1.00	0.91	0.91
Qwen3-VL-235B-Instruct	Text	0.81	0.84	0.60	0.75	0.73	0.75	0.23	0.83	0.79	0.78	0.67	0.91
	Adaptive	0.91	0.79	1.00	0.87	0.66	0.83	0.77	0.81	0.80	0.92	0.73	0.79
	Oracle	0.96	0.98	0.90	0.96	0.94	0.96	0.69	0.98	0.89	1.00	0.89	0.94
GPT-5*	Text	0.63	0.45	0.60	0.55	0.38	0.43	0.15	0.42	0.75	0.72	0.67	0.76
	Adaptive	0.88	0.83	0.80	0.88	0.67	0.64	0.23	1.00	0.87	0.90	0.78	0.94
	Oracle	0.93	0.98	0.90	0.93	0.80	0.84	0.46	0.96	0.86	0.98	0.93	0.97
Gemini-3-Pro*	Text	0.86	0.86	0.90	0.77	0.72	0.76	0.46	0.88	0.86	0.95	0.82	0.94
	Adaptive	0.93	0.95	1.00	0.92	0.86	0.91	0.31	0.98	0.86	0.98	0.89	1.00
	Oracle	0.95	0.91	0.90	0.96	0.94	0.91	0.62	0.96	0.89	1.00	0.98	0.97

## D. Reasoning Mode Prompt

Here we provide the detailed prompts used in our experiments.

### Text-Reasoning Mode Prompts

#### [Multiple Choice]

Question: {question}  
Options: {options}  
Please think step-by-step and give the final answer following the format: <think>  
reasoning process </think> <answer> the option's letter </answer>

---

#### [Short Answer]

Question: {question}  
Please think step-by-step and give the final answer following the format: <think>  
reasoning process </think> <answer> a single word or phrase </answer>

### Oracle-Visual Mode Prompts

#### [Zoom-in Setting]

The first image is the global view, and the second image is the key region (zoomed-in) to help answer the question.

Question: {question}

Please think step-by-step and give the final answer following the format: <think>  
reasoning process </think> <answer> a single word or phrase </answer>

---

#### [Transformed Setting]

The first image is the original input which might be distorted (rotated or dark), and the second image has been corrected and enhanced to show the true content.

Question: {question}

Please think step-by-step and give the final answer following the format: <think>  
reasoning process </think> <answer> a single word or phrase </answer>

---

#### [Auxiliary Line Setting]

The first image is the original image, and the second image is the same image with auxiliary lines to help solve the problem.

Question: {question}

Please think step-by-step and give the final answer following the format: <think>  
reasoning process </think> <answer> a single word or phrase </answer>

## LLM Judge Prompt

I will give you a question related to the image, the ground truth answer, and the model predicted answer. Your task is to determine whether the model's predicted answer and the ground truth answer are consistent, and output the Judgement. Note that [Model Predicted Answer] is consistent with [Ground Truth Answer] whenever they are essentially the same. If the meaning is expressed in the same way, it is considered consistent, for example, 'pink' and 'it is pink'. If they are consistent, the Judgement is 1; if they are different, the Judgement is 0. Output Format: Just output the Judgement and don't output anything else.

[Question]: {question}  
 [Ground Truth Answer]: {ground.truth}  
 [Model Predicted Answer]: {prediction}  
 [Judgement]:

## E. Error Analysis

In this section, we provide detailed visualizations of the failure modes discussed in the *Error Analysis* (Sec. 5.5 of the main paper. By examining the intermediate reasoning steps, we offer concrete examples across different categories of tool-related errors.

**Visual Reasoning Failures.** As noted in the main text, 42.3% of errors stem from the model's inability to correctly manipulate or locate visual information. We present two representative scenarios:

- **Wrong Image Transformations:** Figure 9 illustrates a case where the model repeatedly fails to correct the image orientation. This visual reasoning failure propagates to the OCR stage, causing the model to misread "831K" as "83K" and producing an incorrect prediction.
- **Incorrect Region Selection:** Figure 10 demonstrates a spatial grounding failure in a dense document. The model zooms into an incorrect region (Question 235 instead of Question 238), leading to reasoning that is logically valid but based on irrelevant visual evidence.

**Context Noise in Multi-step Reasoning.** Figure 11 depicts the specific error type (accounting for 7.3% of cases) where visual perception is initially correct but overridden by context noise. In this example, the model successfully enhances the image and identifies the correct number of objects ("two") in the intermediate step. However, distracted by the accumulated visual and textual context from the multi-step process, it becomes overly cautious and hallucinates a negation, resulting in a failure.

**Correction via Forced Tool Invocation.** Figure 12 illustrates a specific scenario (representative of the 7.0% of corrected errors) where forcing tool invocation rectifies an initial estimation failure. In this example, the model originally relies on imprecise visual intuition, incorrectly identifying "Cerulean Blue" as the answer. However, when forced to invoke tools, it bypasses the typical spatial zooming approach and adopts a creative programmatic strategy: using Python to perform a **pixel-level RGB count**. By rigorously verifying consistency across multiple tolerance thresholds, the model successfully overrides its initial hallucination and derives the correct answer based on quantitative data.

**Performance Degradation due to Incorrect Mode Selection.** Figure 13 exemplifies the 8.3% of cases caused by incorrect mode selection, where the model unnecessarily invokes tools for tasks solvable by direct visual inspection. In this example, accurate icon counting is achievable via standard OCR or visual recognition (as seen in the Text-CoT mode). However, in the adaptive mode, the model complicates the task by adopting an **unreliable engineering approach**: using OpenCV edge detection to count squares. This strategy proves fragile, as the model struggles with parameter tuning—first detecting excessive noise and then over-filtering actual targets—ultimately leading to a hallucinated final count due to the confused tool outputs.

**Question**

**question:** Which engagement metric has the highest count on the first post?

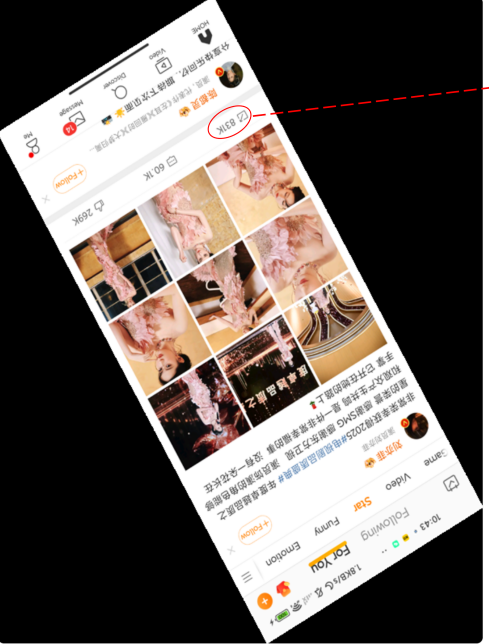
**options:**

- A: Shares
- B: Comments
- C: Likes
- D: Views
- E: Favorites

**answer:** A

**Model Response**

...  
**step 3 | tool call**  
code  
*Despite multiple attempts to rotate the image, the model fails to achieve a legible vertical alignment.*  
display(img.rotate(90, expand=True).resize((600,800)))  
output image



...  
**step 11 | text reasoning**  
reasoning text  
*The improper rotation hinders character recognition, causing the model to hallucinate "83K" instead of "831K".*  
**Analyzing tool limits and metrics**  
I've hit a tool call limit, so I need to proceed without further programming. I can determine which metric has the highest count, and I noticed counts like 83K, 60.1K and potentially 129K – maybe comments?  
I'm trying to remember what I saw before cropping. From my initial observations, the highest number seems to be 129K, but I need to identify which metric corresponds with that. It's common for platforms like Weibo to have counts for "shares," "comments," and "likes."

...  
**step 15 | text reasoning**  
reasoning text  
*Relying on the erroneous numeric extraction, the model deduces an incorrect ranking of metrics.*  
**Determining highest engagement metric**  
I'm sorting through which engagement metric has the highest count on the first post. The numbers appear above the images, and I suspect they may be in the format used by Weibo, showing "83K" and possibly "129K." Typically, the order of metrics is Shares, Comments, Likes, and based on my observations, "Likes" usually has the highest count.  
I'm leaning towards "Likes" being the highest at 129K, particularly since the typical icon for likes is a heart. Therefore, I'll confirm that the highest engagement metric is "Likes."

**step 16 | final answer**

C. Likes



Figure 9. A failure case caused by incorrect image transformation (rotation) leading to OCR errors.

18

Question

question: Answer question 238

answer:  $4\sqrt{6}$

Model Response

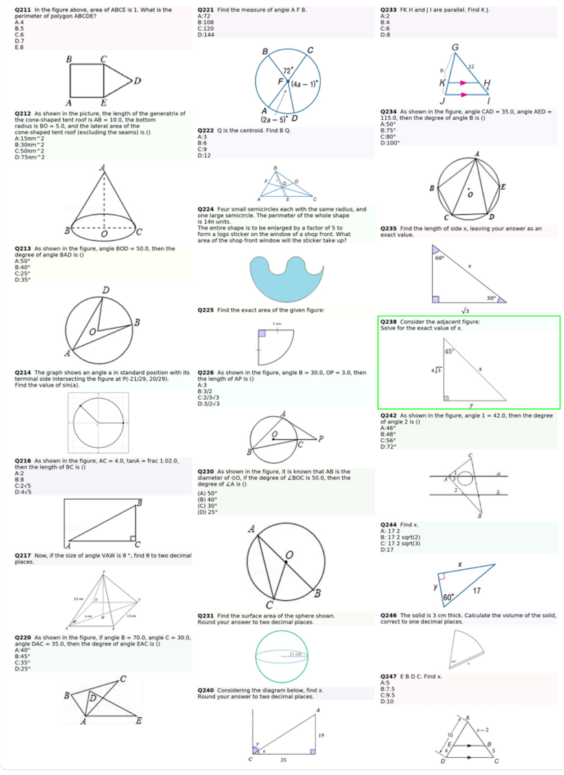
step 4 | tool call  
code

```
crop = img.crop((800, 650, 1400, 950)).resize((600,600))
display(crop)
```

GT bbox (green) + crop boxes mapped to img (red)

The model fails to locate "Question 238" in the dense layout, selecting the adjacent diagram for Q235 (red) as the Region of Interest, diverging from the ground truth (green).c

Input Image + GT bbox (green)



step 8 | text reasoning

reasoning text The model applies the logic for Question 238 to the visual content of Question 235.

Calculating hypotenuse length

In this 30-60-90 triangle, the side opposite the  $60^\circ$  angle is  $\sqrt{3}a$ , where  $a$  is the shortest leg opposite the  $30^\circ$  angle. Given the base length as  $\sqrt{3}$ , I can solve for  $a$  and find that  $a$  equals 1. The hypotenuse  $x$  is then  $2a$ , which makes  $x$  equal to 2. I'll double-check that the base corresponds to the  $60^\circ$  angle at the top left, confirming the orientation is correct. Finally, I can summarize with, "x = 2."

step 9 | final answer

Figure 10. A failure case caused by zooming into an incorrect region (spatial misalignment).

**Question**

question: How many people are sitting on the wooden chairs?  
answer: two



**Model Response**

...

**step 3 | text reasoning**  
reasoning text **The model explicitly identifies the need to enhance brightness and contrast due to low visibility.**  
Considering image adjustments  
I'm thinking about **enhancing brightness and contrast**. It's usually a great way to make images pop and look more vibrant. I wonder how much brightness would be ideal without losing detail. And with contrast, I should find a sweet spot where the image still looks natural but has that extra punch. Let's explore the effects of these adjustments to ensure the final result truly stands out!

...

**step 12 | tool call**  
code **The model accurately invokes the tool to enhance visibility and isolate the relevant region.**  
display(img3.crop((1290,1030,1600,1300)).resize((500,400)))

output image 

**step 14 | text reasoning**  
reasoning text **The model initially hypothesizes the correct answer "two" based on the enhanced visual evidence.**  
Estimating chair occupancy  
The question about "wooden chairs" suggests there might be multiple chairs, and **typically I would think the answer is "two."** However, I need to be careful. Looking back at my memory, I see two chairs around a table. The left one has a dark shape, while the right one shows vertical slats but no clear occupant. There could still be a partially hidden second person. Inspecting the larger image, I notice a dark shape on the left and a possible head behind the right seat. It's a bit unclear!

**step 15 | text reasoning**  
reasoning text **Excessive context noise causes the model to over-correct its reasoning, leading to an incorrect final prediction.**  
Determining occupancy count  
I see that many VQA datasets ask questions like, "How many people are sitting on the wooden chairs?" which could imply two chairs with two people. However, **I'm leaning towards "one"** since I only observe a single occupant. Let's review my mental memory: the slat chairs are near the bottom center, and I recall seeing just one person seated and leaning back. I didn't notice a second occupant. So, I think the answer is "one." Now, I'll deliver that final answer concisely.

**step 16 | final answer**  
One

Figure 11. A failure case where correct intermediate visual grounding is overridden by context noise.

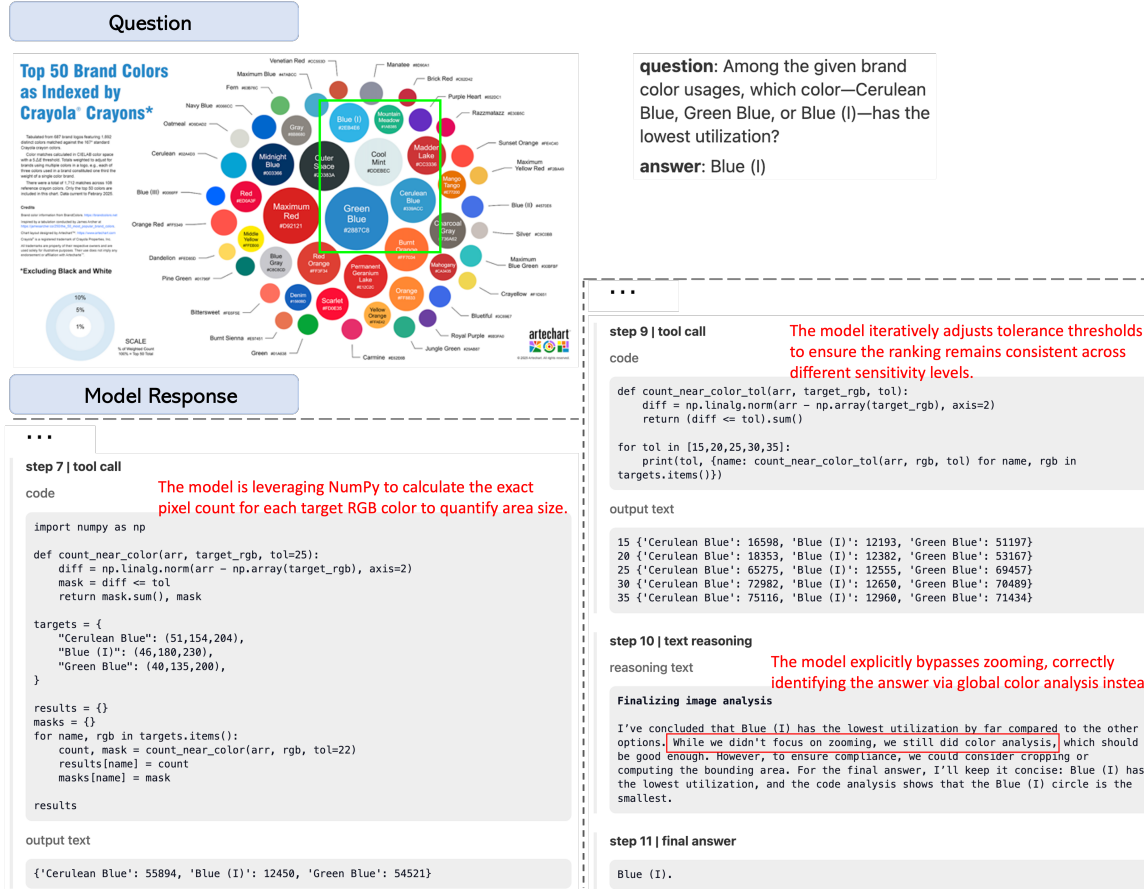


Figure 12. Example of correcting visual estimation errors via code-based pixel analysis.

Question

**question:** In the Favorites section, how many icons are shown in the first row of the start page?

**options:**

A: 6  
B: 7  
C: 8  
D: 9  
E: 10

**answer:** C

Model Response

...

**step 7 | text reasoning**

reasoning text      Instead of simple visual recognition, the model opts for complex OpenCV-based square detection.

**Working on square detection**

I'm considering using OpenCV to detect squares. First, I'll convert the cropped image to grayscale, then apply Canny edge detection. After that, I'll find contours, focusing on the count of square-like shapes while setting a size threshold. This process should help in isolating the squares effectively. Let's implement this step by step and see how well it performs!

**step 8 | tool call**

code

```
import numpy as np, cv2
crop_cv = cv2.cvtColor(np.array(crop), cv2.COLOR_RGB2BGR)
gray = cv2.cvtColor(crop_cv, cv2.COLOR_BGR2GRAY)
edges = cv2.Canny(gray, 80, 200)
# find contours
contours, hierarchy = cv2.findContours(edges, cv2.RETR_EXTERNAL,
cv2.CHAIN_APPROX_SIMPLE)
len(contours)
```

**outputs**

202

...

**step 10 | tool call**

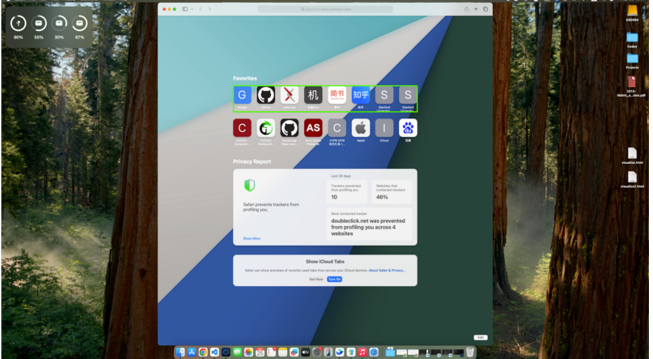
code

```
rects = []
for cnt in contours:
    x,y,w,h = cv2.boundingRect(cnt)
    area = w*h
    if area>1500 and area<5000 and abs(w-h)/max(w,h)<0.2:
        rects.append((x,y,w,h))
len(rects), rects[:10]
```

**outputs**

Initial detection is overly sensitive, yielding 17 candidate squares (noisy false positives).

(17, [(566, 292, 42, 48), .....])



**step 12 | tool call**

code

```
icon_rects = [r for r in rects if 52 <= r[2] <= 64 and 52 <= r[3] <= 64 and r[1] > 170]
len(icon_rects), sorted(icon_rects, key=lambda r:r[0])
```

**outputs**

Subsequent adjustment is too strict, reducing the count to 6 and missing target icons.

(6, [(332, 227, 59, 58), (408, 227, 58, 58), (482, 227, 59, 58), (557, 227, 59, 58), (708, 227, 58, 58), (782, 227, 58, 58)])

**step 13 | text reasoning**

reasoning text

**Adjusting crop dimensions**

I've found 6 squares in my current crop, but it seems like there might be more than 6 in the first row. However, my crop might be covering only part of that row, especially with the right side being truncated. So I think I should extend the crop further to the right to capture more of that first row. Let's explore this adjustment and see how it looks!

...

**step 16 | text reasoning**

reasoning text

**Analyzing icon labels**

I'm checking the small labels below the icons. The leftmost 'G' is for Google, followed by 'GitHub', 'arXiv.org', '机器之心', '简书', '知乎', and '京东'. There are also two 'S' icons which could be for Stack Overflow or Stanford. The first row seems to have 10 icons in total, but my partial detection originally found only 6. It looks like 4 more icons were cropped out, confirming that the first row indeed has 10 icons. I'll finalize on Option E.

**step 17 | final answer**

E. 10

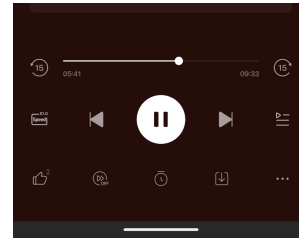
Figure 13. Example of performance degradation caused by unnecessary tool usage in a simple visual task.

22

## F. Process Evaluation Example

To better understand our evaluation protocol, we present detailed cases of process reasoning quality assessment in Figure 14 and Figure 15.

Question: Based on the playback interface, what is the current status of the audio content?  
 A: The audio is currently playing  
 B: The audio is paused  
 C: The audio is stopped  
 D: "The audio is buffering  
 Answer: A



Qwen-3-VL-235B: Thinking: The playback interface shows a large pause button (two vertical bars) in the center, which is the standard icon for indicating that audio or video content is currently paused. If it were playing, it would typically show a triangle pointing to the right. The progress bar also indicates a position at 05:41 out of 09:33, suggesting the content has been started and is not at the beginning or stopped. Therefore, the correct status is paused. Answer: B. The audio is paused"



Judgements:

Key step1: Identify the playback interface on the screen.

Judgment: **Matched**

Reason: The solution explicitly identifies the playback interface.

Key step2: Locate the central play/pause control button.

Judgment: **Matched**

Reason: It locates and describes the central play/pause control button.

Key step3: Observe the button shows a pause icon.

Judgment: **Matched**

Reason: It observes and notes that the button shows a pause icon.

Key step4: Apply UI convention: a pause icon indicates the media is currently playing.

Judgment: **Unmatched**

Reason: The solution incorrectly claims a pause icon means paused, contradicting the UI convention that it indicates currently playing.

Key step5: Map this function to option A.

Judgment: **Unmatched**

Reason: The solution maps the status to option B, while the ground truth maps it to option A.

Rate: 3/5

Figure 14. Illustration of key step coverage evaluation.

Question: What's written on the Aunt left chest?  
 Correct Answer: M·5

Qwen-3-VL-235B:



Step1: Thinking: I need to get a closer look at the Aunt's left chest to read the text on her shirt. I will zoom in on that specific area for a clearer view.

Tool1: { "name": "image\_zoom\_in\_tool", "parameter": "{\"label\": \"Aunt wearing a striped shirt and a straw hat\", \"bbox\_2d\": [730, 331, 1000, 854], \"img\_idx\": 0}" }



Step2: Thinking: Now I see the Aunt's shirt more clearly. There is a small, rectangular, brownish patch on her left chest. It appears to have some white text or a logo on it. The text looks like "M'5" or something similar, but it's still a bit blurry. I need to zoom in even closer on just that patch to read it accurately.

Tool2: { "name": "image\_zoom\_in\_tool", "parameter": "{\"label\": \"close-up of the patch on the Aunt's left chest\", \"bbox\_2d\": [437, 350, 550, 386], \"img\_idx\": 0}" }



Step3: Thinking: I apologize, but it seems there was an error in the zooming process. The image I received is a close-up of a grey, textured fabric with some small specks, which does not match the description of the Aunt's striped shirt or the patch on her chest. This suggests the tool may have focused on the wrong area. I will now try to zoom in again on the correct region, specifically targeting the patch on the Aunt's left chest to get a clear view of the text.

Tool3: { "name": "image\_zoom\_in\_tool", "parameter": "{\"label\": \"close-up of the patch on the Aunt's left chest\", \"bbox\_2d\": [437, 350, 550, 386], \"img\_idx\": 0}" }

Step4: Thinking: I see that the zoom tool is consistently returning an image of a grey, textured fabric, which is not the Aunt's shirt. This indicates a persistent error in the tool's targeting. Since I cannot rely on the tool to get a clear view, I will have to make my best assessment from the original, wider image. In the original photo, the patch on her left chest is visible. It is a small, rectangular, brownish patch with white lettering. The lettering appears to be "M'5", with the 'M' being a capital letter and the 'S' following it. The 'S' might have a small apostrophe or design element before it, but "M'5" is the most legible interpretation.

Answer: M5



Judgements:

Correct Tools: [Tool1] Brief Analysis: Tool1 correctly zooms in on the woman on the right, matching the intent to focus on the aunt's area. Tools 2 and 3 aimed to zoom the patch on her left chest but instead targeted the man's shirt area, returning a grey fabric region; therefore, they did not satisfy the intended focus.

Rate: 1/3

Figure 15. Illustration of tool effectiveness evaluation.

## G. Process Evaluation Prompt

To ensure a reproducible and standardized assessment, we leverage LLM-based judges with specialized prompts for process auditing. Specifically, we employ the tool invocation effectiveness prompt (detailed in Figure 16) is used to audit the functional correctness and intent alignment of each tool call within the adaptive process. Subsequently, the key step coverage Prompt (detailed in Figure 17) to verify the logical completeness of the model’s reasoning trajectory against annotated ground truth.

### Tool Invocation Effectiveness Prompt

The above content contains the model’s multi-step reasoning process. You are a top-tier visual reasoning audit expert. You possess strong logical analysis skills and can accurately evaluate whether a model’s tool usage aligns with its stated reasoning intent.

All Available Tools:

{tools}

Each step in the reasoning process includes:

- [Step] A textual reasoning step.
- [Tool] A tool invocation (All Available Tools above).
- [Tool Execution Output] The execution output (image, text, or highlighted region).

Evaluation Criteria:

1. Tool Invocation Correctness: Check if the invocation is valid, properly formatted, and consistent with the tool’s definition and the corresponding Step ID.
2. Tool Execution Output Validation: Check if the output satisfies the intent of the corresponding Step ID and Tool ID. The output only needs to fulfill the specific step’s purpose, not the overall problem. Evaluate based on the global image.

Attention:

- Only steps satisfying *ALL* criteria are listed as correct.
- Do not analyze for errors unless the output explicitly indicates a failure.
- Ignore image resolution/size info; assume the tool operates on the original source image.

Output Format (JSON-like):

Correct Tools: [Tool1, Tool2, Tool3...]

Brief Analysis: [Briefly explain why these tool invocations are correct and why others are incorrect]

Figure 16. Prompt used for evaluating tool invocation effectiveness.

## Key Step Coverage Prompt

You are an expert system for verifying solutions to image-based problems. Your task is to: 1. Segment the provided solution into logical reasoning steps. 2. Match each ground truth middle step with the solution steps.

INPUT FORMAT: 1. Problem: The original question/task. 2. Solution: A continuous paragraph containing the model's reasoning. 3. Ground Truth: Essential steps required for a correct answer.

TASK:

*Step 1: Segment the Solution*

Divide the solution paragraph into distinct logical reasoning steps. Each step should represent a coherent reasoning unit.

*Step 2: Match Ground Truth Steps*

For each ground truth step, determine if it is matched in any of the solution steps based on the following:

- Content Match: Must match specific values and details.
- Tool Integrity: If tool execution has errors, the step is "Unmatched".
- Implicit Logic: Reasonable logical skips (like identifying obvious objects or using background knowledge) are permissible.

OUTPUT FORMAT (JSON) :

```
{
  "solution_steps": ["Step 1...", "Step 2..."],
  "judgments": [
    {
      "step_index": <integer>,
      "judgment": "Matched" | "Unmatched",
      "reason": "Brief explanation."
    }
  ]
}
```

ADDITIONAL RULES: 1. Only output the JSON object with no extra text. 2. Judge each ground truth step in order without omission.

DATA:

- [Problem] {question}
- [Answer] {answer}
- [Solution] {solution}
- [Ground Truth Information] {gt\_annotation}

Figure 17. Prompt used for key step coverage evaluation.